Orbital: The Electronic Journal of Chemistry
journal homepage: www.orbital.ufms.br
ISSN 1984-6428

| Vol 7 | | No. 3 | | July-September |

Full Paper

Isotherm Studies of Equilibrium Sorption of Cu^{2+} and Cd^{2+} from Aqueous Solutions by Modified and Unmodified Breadfruit Seed Hull

Christopher Uchechukwu Sonde[a*], Stevens Azubuike Odoemelam[b] and Francis Kalu Onwu[b]

[a]*Department of Chemistry/Biochemistry/Molecular Biology, Federal University, Ndufu-Alike Ikwo, P.M.B 1010 Abakaliki, Ebonyi State, Nigeria.*
[b]*Department of Chemistry, Michael Okpara University of Agriculture, Umudike, P.M.B 7267, Umuahia, Abia State Nigeria.*

Article history: Received: 01 October 2014; revised: 30 January 2015; accepted: 17 March 2015. Available online: 13 September 2015. DOI: http://dx.doi.org/10.17807/orbital.v7i3.625

Abstract: The ability of an economically cheap adsorbent material of natural origin, African breadfruit seed hull, was assessed for Cu(II) and Cd(II) ions' adsorption from aqueous solutions. The effects of adsorbent dose, particle size and initial metal ion concentrations were investigated in a batch adsorption process. The experimental data were analyzed using five two-parameter isotherm equations (i.e., Langmuir, Freundlich, Temkin, Harkins-Jura and Halsey isotherm models). Freundlich and Halsey models provided the best description for the adsorption data while the other three models gave fairly good interpretation to the experimental adsorption data. The maximum adsorption capacity corresponding to saturation of sites (q_{max}), obtained from the Langmuir plots, were 7.76 and 8.06 mg g^{-1} for Cu(II) and Cd(II) onto the unmodified breadfruit seed hull (UBSH) and 12.67 and 13.97 mg g^{-1}, respectively for Cu(II) and Cd(II) adsorption onto the modified breadfruit seed hull (MBSH). The experimental results showed that there was an enhancement in the removal of the metal ions by the mercaptoacetic acid-modified breadfruit seed hull.

Keywords: adsorption capacity; adsorption isotherms; metal ions; modified breadfruit seed hull; unmodified breadfruit seed hull

1. INTRODUCTION

Pollution of our environment by heavy metals has become a developing ecological problem and is currently a big concern and a subject of many current researches [1]. Heavy metals are continuously released in large concentrations during processes like electroplating, metal finishing, metallurgical, chemical manufacturing and mining. Some of these heavy metal ions such as mercury, lead, cadmium, nickel, copper, zinc, chromium *etc*. have significant impact on the environment. They are greatly toxic as ions or in the form of compounds; soluble in water and are readily absorbed into living tissues. Presence of heavy metals such as chromium, cadmium, arsenic, mercury, lead, nickel and copper has been known to cause serious damaging effect to human body [2]. Concentrations of 0.005 mg L^{-1} (for Pb^{2+} and Cr^{3+}), 0.1 mg L^{-1} (for Cu^{2+}), 0.001 mg L^{-1} (for As^{5+}, Cd^{2+} and Ni^{2+}) have been observed to cause illness in humans and can even be fatal [3].

Of all the conventional techniques that have been employed for toxic metals removal from aqueous solutions such as coagulation, precipitation, ion-exchange, electrochemical methods, membrane processes, extraction, adsorption, *etc* [4, 5], adsorption is currently been considered as the most suitable technique because of its simplicity in terms of process design and cost effectiveness. Some novel materials applied as adsorbents for removal of metal ions from solutions include: biomaterials [6-15], zeolites [16], activated carbons [17-21], clay materials[22, 23], polymeric materials [24, 25], Schiff bases immobilized on silica support [26-31] and nanomaterials [32-37].

Among these adsorbents, agricultural waste materials have proven a viable option for wastewater decontamination due to their unique composition, availability in abundance, renewability, low cost, high efficiency and eco-friendliness. The present study is concerned with the removal of Cu(II) and Cd(II) ions from aqueous solutions using a common agricultural

*Corresponding author. E-mail: xtopheraries@yahoo.co.uk

waste, the seed hull of African breadfruit. The effects of various process parameters, namely, particle size, adsorbent mass and initial metal ion concentration on the removal of these metal ions were investigated. The overall efficiencies of the modified and unmodified adsorbents were tested using different adsorption isotherm models.

2. MATERIAL AND METHODS

2.1. Preparation of Adsorbent

African breadfruit (*Treculia africana*) seed hulls were obtained from Uturu, Abia State, Nigeria. The hulls were cut into small pieces, air-dried and crushed into powdery forms using a manually-operated blender. The breadfruit seed hull meal obtained was further dried in the oven at 50 ^{o}C for 12 h. Afterwards, it was removed from the oven and sieved through different sieve sizes, 250, 425 and 600 µm mesh screens.

2.2. Activation of Adsorbent

The breadfruit seed hulls in different particle sizes were further soaked in dilute nitric acid solution (2% v/v) overnight at a temperature of 29 ^{o}C. After 24 h, the meal was filtered through a Whatman No. 41 filter paper and rinsed with deionized water and air-dried. The adsorbent was dried again in the oven at 105 ^{o}C for 6 h. After drying, the hulls were divided into two parts; one part was used for adsorption studies without chemical modification (i.e. the unmodified breadfruit seed hull) and was labeled as UBSH while the second portion was modified by the introduction of thioglycolic acid (*i.e*. the modified breadfruit seed hull labeled as MBSH).

2.3. Modification of Adsorbent

The African breadfruit (*Treculia africana*) seed hull was thiolated by the method reported by Okieimen and Okundaye [38]. Specifically, a 25 g sample of the activated breadfruit seed hulls was thiolated with 250 mL of 1.0 M solution of thioglycollic acid for 24 h at 29 ^{o}C. The mixture was filtered after 24 h, washed with deionized water and then with methanol. It was finally washed with deionized water and dried at 50^{o}C for 12 h. This thioglycolic acid modification process led to the thiolation of the hydroxyl groups of the cellulosic biomass by the following reaction:

Biomass–OH + $HSCH_2CO_2H \rightarrow$ Biomass–SH + $CH_3CO_2^- + H^+$

The degree of thiolation was estimated titrimetrically by reaction of the thiolated hull with iodine and back-titration of the unreacted iodine with sodium thiosulfate solution. The degree of thiolation obtained from the titration work is 2.71%.

2.4. Preparation of the Adsorbates

All reagents used were of analytical grade and were used as purchased without further purification. Doubly-distilled and deionized water was used in the preparation of all sample solutions. Stock solutions of Cu^{2+} and Cd^{2+} of 1000 mg L^{-1} concentrations were prepared by dissolving known amounts of copper nitrate [$Cu(NO_3)_2.6H_2O$] and cadmium chloride ($CdCl_2$) respectively in 1000 mL of deionized water. From the stock solutions, working solutions (aliquots) of 10mg/L - 80 mg L^{-1} (initial concentrations) of each metal ion were prepared by serial dilution.

2.5. Sorption Studies

Sorption studies for Cu^{2+} and Cd^{2+} were carried out for each adsorbent (UBSH and MBSH respectively) at pH 6, temperature, 30 ^{o}C, and at the varying initial concentrations by transferring 50 mL standard solution of each metal ion into five 250 mL Erlenmeyer flasks. An accurately weighed sample of 1 g of each adsorbent was weighed into each of the flasks and agitated for 2 h to attain equilibrium. An X21 – 0014 KERN 770 –15 analytical balance, made in Germany, was used. The balance measures to an accuracy of 0.0001g.

At the end of the equilibration time, each flask was filtered rapidly and the filtrates were collected into various sample bottles. The residual (equilibrium) concentration of the filtrates of each metal solution was analyzed using UNICAM 969 solar atomic absorption spectrophotometer (AAS).

2.5.1 Data Analysis

Experimental readings were carried out in triplicates and the average of each reading was used in the calculations. The amount of Cu^{2+} and Cd^{2+} from each metal solution adsorbed at equilibrium was computed using mass balance equation as shown in equation (1):

$$q_e = (C_0 - C_e)\frac{V}{m} \quad (1)$$

where q_e is the amount of metal ion adsorbed at equilibrium *i.e.*, sorption capacity in mg/g; C_o is the initial metal ion concentration (mg L^{-1}); C_e is the metal ion concentration at equilibrium, *i.e.*, the final concentration of metal ion in solution after adsorption (mg L^{-1}); V is the volume of the initial metal ion solution used which is constant (50mL) and m is the mass of adsorbent used (*i.e.* 1 g).

3. RESULTS AND DISCUSSION

3.1 Effect of particle size

Figs. 1 and 2 show that the adsorption capacity of the metal ions decreased with increase in particle size from 250 µm to 600 µm for both metal ions onto the two adsorbents. However, maximum adsorption capacities for the two metal ions by the adsorbents occurred at a particle size of 250 µm at a constant pH 5 and at an initial concentration of 100 mg L^{-1}. The higher percentage adsorption with smaller particle sizes may be attributed to the fact that smaller particle sizes provide a larger surface area. The high rate of adsorption by adsorbents with smaller particle sizes had been generally attributed to the availability of more adsorption sites resulting from increase in specific surface areas of the adsorbents. Results further show that the mercaptoacetic acid-modified surface exhibited a greater adsorption for the metal ions than the unmodified breadfruit seed hull. The equilibrium time was also found to remain unaffected by the change in adsorbent particle size.

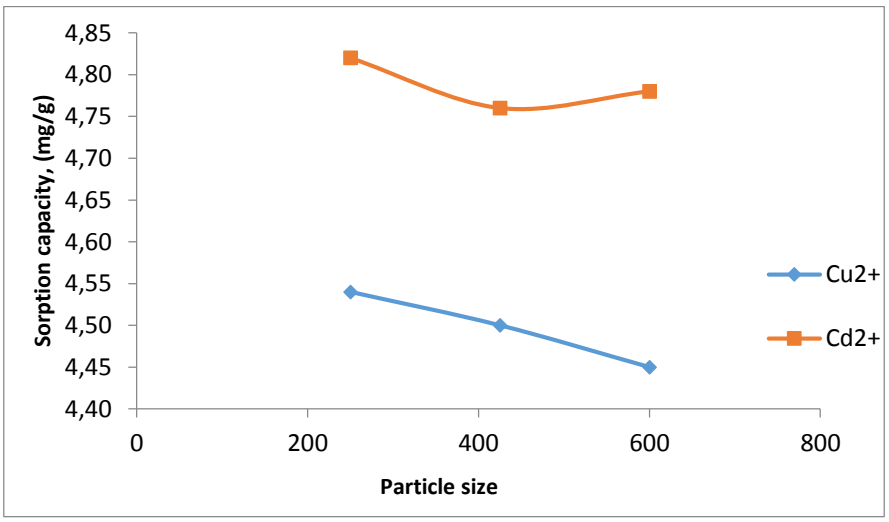

Figure 1. Variation of sorption capacity with particle size for adsorption of the metal ions onto UBSH.

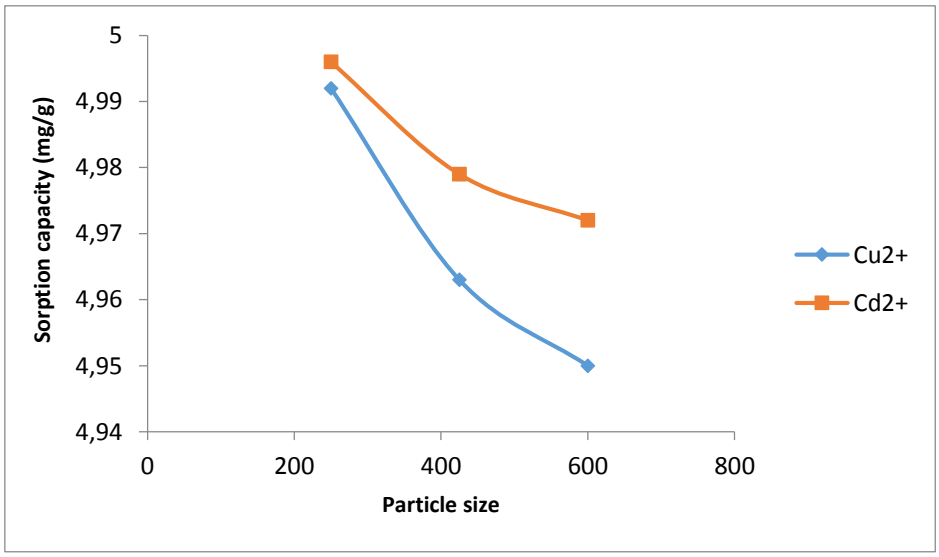

Figure 2. Variation of sorption capacity with particle size for adsorption of the metal ions onto MBSH.

3.2 Effect of Adsorbent Dose

To investigate the effect of adsorbent dosage (mass), the adsorption of the metal ions, Cu(II) and Cd(II) onto the unmodified and modified African breadfruit seed hull was measured at four different adsorbent concentrations (1, 2, 5 and 10 g L^{-1}) for initial metal ion concentration of 100 mg L^{-1}. The removal efficiencies of the metal ions by the adsorbents are shown in Figures 3 and 4 while the equilibrium amount adsorbed are presented in Figures 5 and 6. From Figures 3 and 4, it is clear that Cu^{2+} and Cd^{2+}percentage removal increases with increasing adsorbent concentration. This may be due to the presence of more active adsorption sites for Cu^{2+} and Cd^{2+} at higher adsorbent concentrations. After the adsorbent dose had exceeded 2 g L^{-1}, no obvious increase was observed and this suggests that the equilibrium between metal ions bound to the adsorbent and free ions in the bulk phase is established. A similar observation had been recorded by Babel and Kurniawan [39] and Nomanbhay *et al*. [40]. Figures 5 and 6 show that Cu^{2+} and Cd^{2+} adsorption capacities (*i.e.*, amount adsorbed per unit mass of the adsorbent) decreased as adsorbent concentration increases. This shows that more active sites are utilized at lower adsorbent concentration, while at higher adsorbent dosage, only part of the active sites are occupied by Cu^{2+} and Cd^{2+} leading to a lower adsorption capacity and a similar observation had been recorded by Li *et al*. [41]. Figs. 3-6 show in general that the percentage removal of these metal ions increased with increasing adsorbent dosage while the amount adsorbed per unit mass decreased and became almost constant at higher dosage > 2.0 g/L. The increase in percentage removal of these heavy metals with increasing adsorbent dose is due to the greater availability of the exchangeable sites or surface area while the decrease in adsorption uptake with increasing adsorbent dosage is mainly due to the unsaturation of adsorption sites through the adsorption reaction.

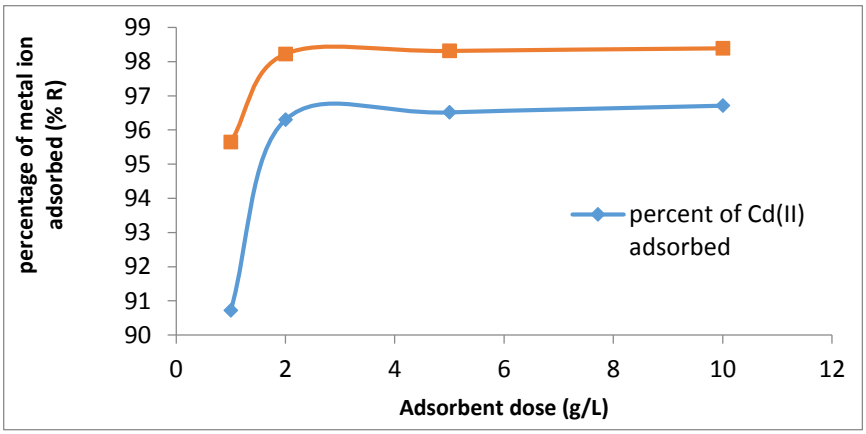

Figure 3. Effect of adsorbent dose on the percentage of metal ions adsorbed by UBSH. Conc. = 80 mg L^{-1}; pH = 6.0; Temp. = 30 ºC; contact time = 120 min.

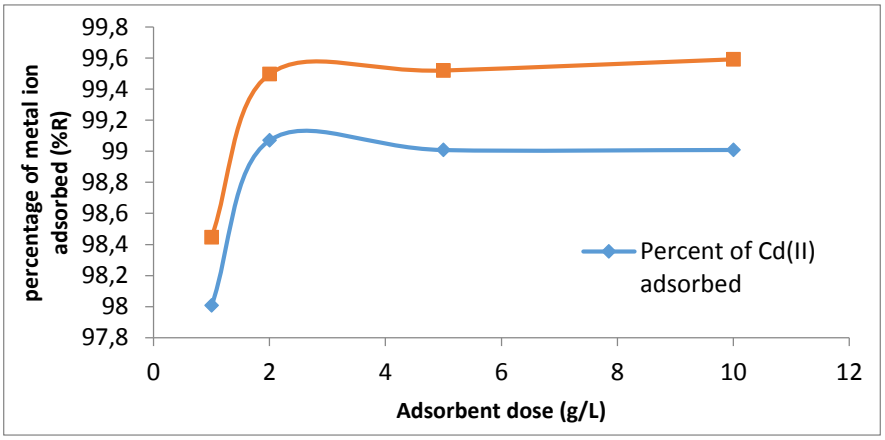

Figure 4. Effect of adsorbent dose on the percentage of metal ions adsorbed by MBSH. Conc. = 80 mg L^{-1}; pH = 6.0; Temp. = 30 ºC; contact time = 120 min.

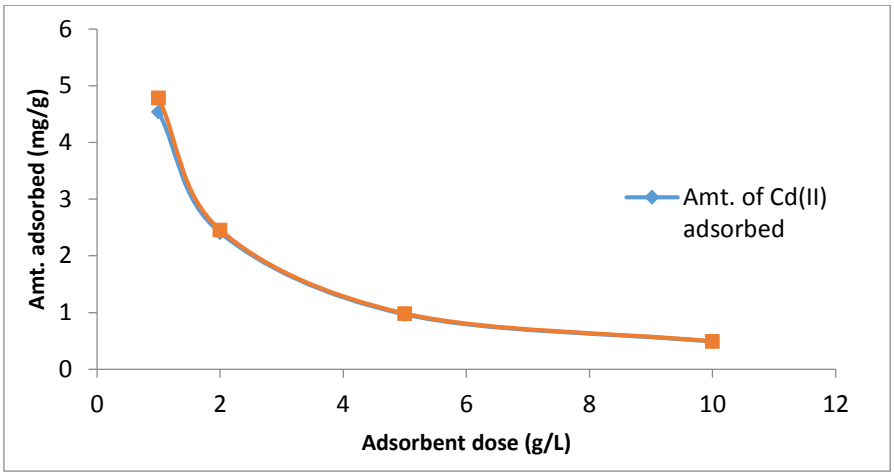

Figure 5. Effect of adsorbent dose on the amount of metal ionsadsorbed by UBSH. Conc. = 80 mg L^{-1}; pH = 6.0; Temp. = 30 °C; contact time = 120 min.

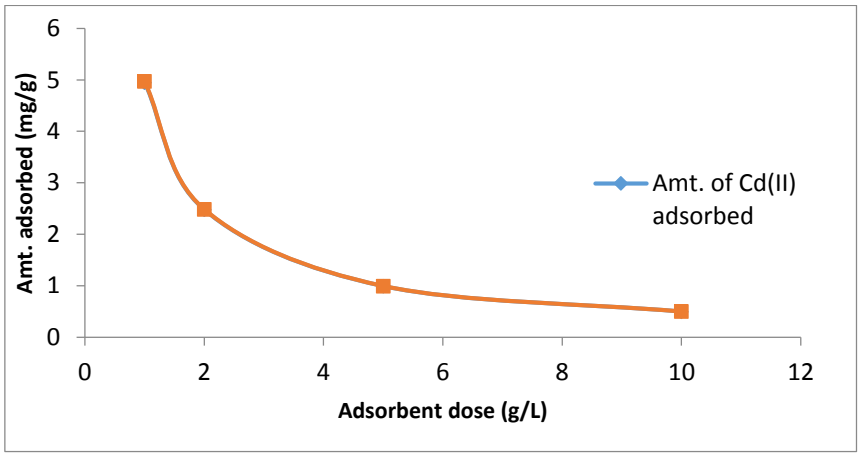

Figure 6. Effect of adsorbent dose on the amount of metal ions adsorbed by MBSH. Conc. = 80 mg L^{-1}; pH=6.0; Temp. = 30 °C; contact time = 120 min.

3.3 Adsorption Isotherms

Adsorption Isotherms relate the amount of metal ions adsorbed at equilibrium per unit mass of the adsorbent, (mg g^{-1}), to the concentration of the metal ions, C_e (mg L^{-1}). The Langmuir, Freundlich,Temkin, Harkins-Jura and Halsey isotherm models have been employed in this study to interpret the adsorption data.

3.3.1 The Langmuir Isotherm

The Langmuir isotherm may be represented as follows:

$$q_e = \frac{q_{max} k_L C_e}{1 + k_L C_e} \qquad (2)$$

Where q_e is the adsorption capacity in mg of adsorbate per gram of adsorbent, C_e is the equilibrium metal ion concentration in solution, q_{max} is the maximum adsorption capacity corresponding to monolayer coverage and K_L is the Langmuir Isotherm constant.The linear form of the Langmuir isotherm equation aids in the evaluation of the maximum adsorption capacity (q_{max}) corresponding to monolayer coverage (or site saturation) and the Langmuir constant, K_L of the adsorption process and is represented as:

$$\frac{C_e}{q_e} = \frac{1}{q_{max} K_L} + \frac{C_e}{q_{max}} \qquad (3)$$

The Langmuir constant, K_L expresses the affinity of the adsorbent binding sites for the metal ions. The values of q_{max} and K_L were calculated from the slope and intercept of the linear plots of C_e/q_e vs C_e

(Figures 7 and 8) and are presented in Table 1.

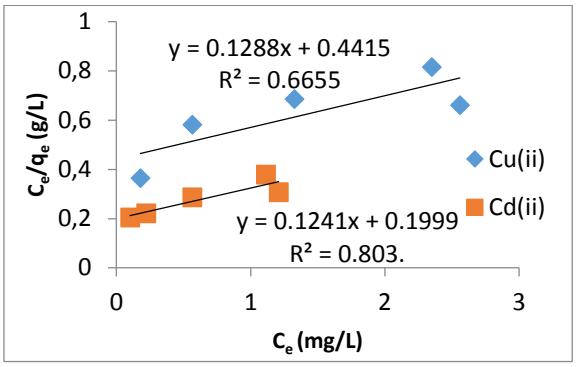

Figure 7. Langmuir isotherm plot for adsorption of the metal ions from aqueous solutions by UBSH.

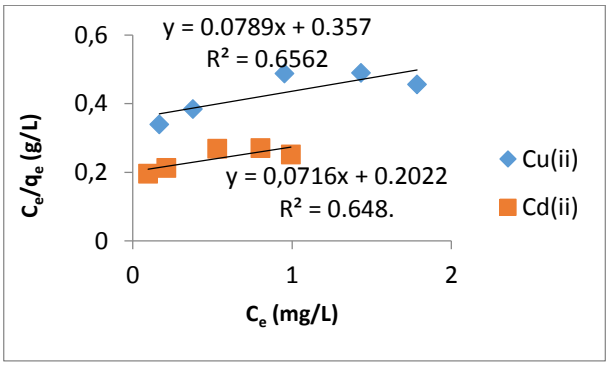

Figure 8. Langmuir isotherm plot for adsorption of the metal ions from aqueous solutions by MBSH.

The low correlation coefficients (R^2 values) obtained showed that the Langmuir isotherm does not give a perfect fit for the adsorption data. The q_{max} values obtained for the metal ions on the adsorbent showed a greater removal for Cd(ll) than Cu(ll) and also showed that the modification of the adsorbent by thioglycollic acid further showed an enhanced removal due to the incorporation of thiol group (-SH) into the adsorbent surface(Table 1).

The essential characteristics of the Langmuir isotherms can be expressed in terms of a dimensionless quantity called separation factor (or equilibrium parameter) R_L, defined as [42],

$$R_L = \frac{1}{(1+K_L C_o)} \qquad (4)$$

where K_L is the Langmuir constant and C_0 is the initial concentration of the metal ions (mg L^{-1}). The R_L values indicate the shape of the isotherm. According to McKay *et al*. [43], R_L values between 0 and 1 indicate favourable adsorption, while R_L value equal to 0 indicate irreversible adsorption, R_L = 1, linear and R_L> 1 indicates unfavourable adsorption.

The values of $R_L$obtained for the adsorption of the two metal ions; Cu(II) and Cd(II) by the adsorbents were all less than unity (Table 1) indicating that the isotherms were favourable under the conditions of this study.

Table 1. Langmuir Isotherm Constants for adsorption of Cu(II) and Cd(II) ions by the adsorbents.

Constants	UBSH		MBSH	
	Cu(II)	**Cd(II)**	**Cu(II)**	**Cd(II)**
K_L (L mg^{-1})	29.19 x 10^{-2}	62.07 x 10^{-2}	22.11 x 10^{-2}	35.40 x 10^{-2}
q_{max} (mg g^{-1})	7.76	8.06	12.67	13.97
R_L	0.04	0.02	0.05	0.03
R^2	0.6655	0.8037	0.6562	0.6487

3.3.2 The Freundlich Isotherm

The Freundlich model was introduced to study the adsorption intensity of the adsorbates towards the adsorbents. The linear form of the Freundlich adsorption isotherm is expressed as:

$$\ln q_e = \ln K_F + \frac{1}{n} \ln C_e \qquad (5)$$

where K_F and n are Freundlich constants. The plots of ln q_e vs ln C_e yielded straight lines with high correlation coefficients thus indicating the fitting of the adsorption data into Freundlich isotherm (Figures 9 and 10). The constants K_F and 1/n were calculated from the intercept and slope of the straight line plots and are presented in Table 2. K_f depicts the ease of removal of the adsorbates, (Cu^{2+} and Cd^{2+}) from aqueous solutions. The n values give information on the favourability and capacity of the adsorbent/adsorbate system and values between 1 and 10 have been found to depict favourable adsorption conditions [44]. The values obtained in our study (Table 2) show beneficial adsorption for the

system. According to Anusiem *et al.* [44], the fit of experimental adsorption data to Freundlich model shows that the mode of adsorption of the metal ions by the adsorbents follows physical adsorption. The high R^2 values obtained in our study show a fit of the experimental data into Freundlich model.

Table 2. Freundlich isotherm constants for adsorption of Cu(II) and Cd(II) ions by the adsorbents.

Constants	UBSH		MBSH	
	Cu (II)	Cd (II)	Cu (II)	Cd (II)
K_F	1.615	3.068	2.214	3.690
N	1.334	1.280	1.178	1.158
R^2	0.9904	0.9894	0.9950	0.9954

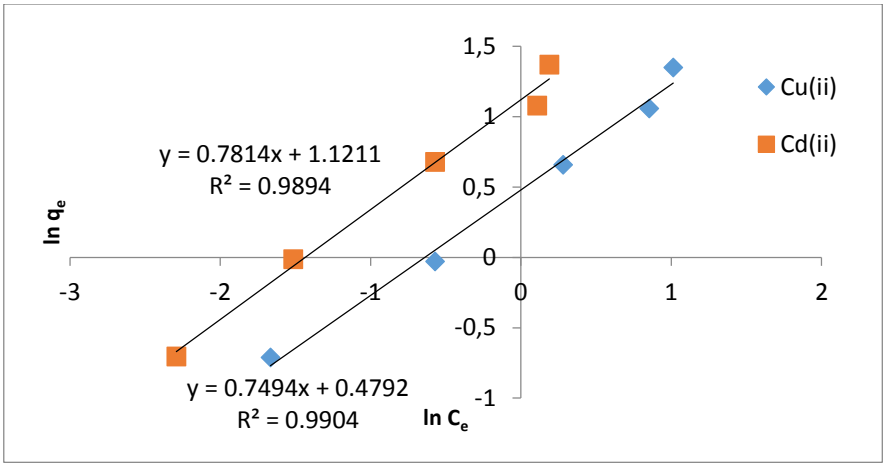

Figure 9. Freundlich isotherm plot of ln q_e *vs* ln C_e for the adsorption of the metal ions from aqueous solutions by UBSH.

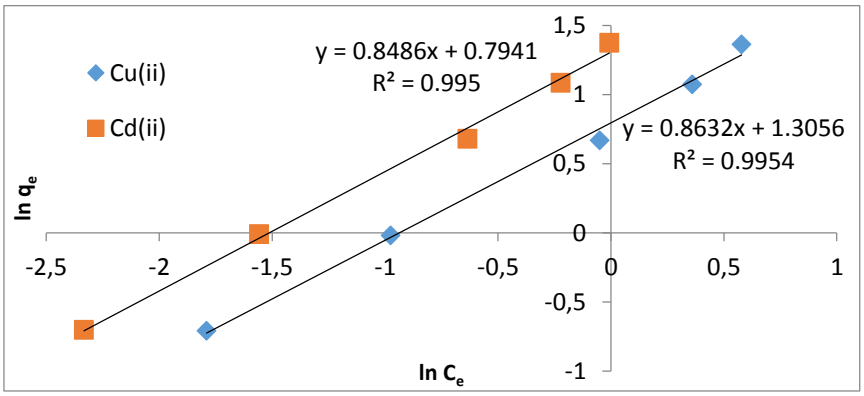

Figure 10. Freundlich isotherm plot of ln q_e *vs* ln C_e for the adsorption of the metal ions from aqueous solutions by MBSH.

3.3.3 Temkin Isotherm

The Temkin isotherm model is a vital tool for estimating the adsorption heat and is evaluated using the following equation [45, 46]:

$$q_e = \frac{RT}{b_T}\ln(K_T C_e) = B_T \ln(K_T C_e) \qquad (6)$$

where the constant $B_T = RT/bT$ is related to the adsorption heat, R is the gas constant (8.314 J/mol K), T(K) is absolute temperature in Kelvin, bT (J mol^{-1}) is the Temkin isotherm constant, which is the variation of adsorption energy and K_T is the equilibrium binding constant corresponding to the maximum binding energy.

The linear Temkin isotherm model equation is given as:

$$q_e = \frac{RT}{b_T}\ln k_T + \frac{RT}{b_T}\ln C_e \qquad (7)$$

Both b_T and K_T can be calculated from the slope and the intercept of the linear plot based on q_e *versus* $ln(C_e)$, respectively. Figs. 11 and 12 show the Temkin isotherm plots for Cu(II) and Cd(II) adsorption onto the unmodified and thiolated surfaces. The Temkin constants and the coefficients of correlation (R^2 values) are presented in Table 3. The lower R^2 values as compared to Freundlich isotherm suggest that the Temkin isotherm model gave a fairly good description for the experimental data. The values of adsorption heat for the metal ions on both unmodified and thiolated surfaces ranged from 1.314 kJ mol^{-1} to 2.202 kJ mol^{-1} (Table 3).

Table 3. Temkin isotherm constants.

Constants	UBSH		MBSH	
	Cu(II)	Cd(II)	Cu(II)	Cd(II)
K_T	1.818	1.601	1.911	2.459
b_T	2201.85	1314.31	1885.16	1832.24
R^2	0.8536	0.9126	0.8951	0.8998

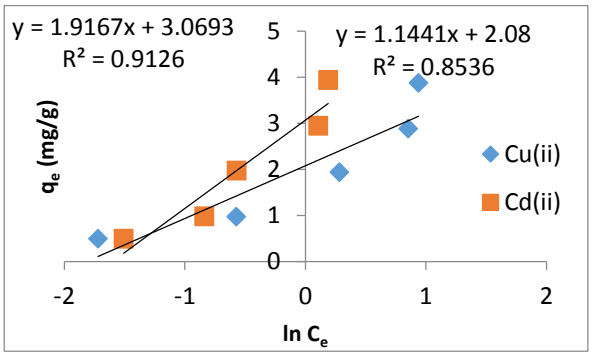

Figure 11. Temkin isotherm plot of q_e *vs* ln C_e for adsorption of the metal ions onto UBSH.

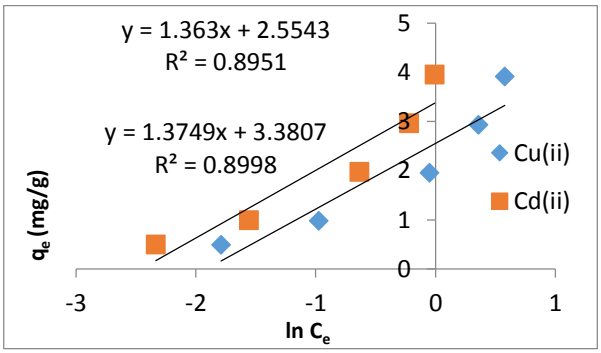

Figure 12. Temkin isotherm plot of q_e *vs* ln C_e for adsorption of the metal ions onto MBSH

3.3.4 Harkins-Jura Isotherm model

Harkins-Jura isotherm model mainly describes the multilayer adsorption and the existence of the heterogeneous pore distribution in the surface of adsorbents.

The Harkins-Jura isotherm equation is usually expressed as [45, 46]:

$$\left[\frac{1}{q_e^2}\right] = \left[\frac{B_{HJ}}{A_{HJ}}\right] - \left[\frac{1}{A_{HJ}}\right] log(C_e) \qquad (8)$$

Where B_{HJ} and A_{HJ} are the Harkins-Jura constants. Both A_{HJ} and B_{HJ} can be achieved from the slope and the intercept of the linear plots of $\left[\frac{1}{q_e^2}\right]$ versus $log(C_e)$ respectively. The Harkins-Jura isotherm plots for the Cu(II) and Cd(II) adsorption on the adsorbents is presented in Figs. 13 and 14 and the relevant isotherm constants are calculated and presented in Table 4. It can be observed from Table 4 that the low R^2 values signify a poor fit of the isotherm model to the experimental adsorption data. This result reveals that Cu(II) and Cd(II) adsorption on the adsorbents did not involve a multilayer adsorption.

Table 4. Harkins-Jura Isotherm Constants.

Constants	UBSH		MBSH	
	Cu(II)	Cd(II)	Cu(II)	Cd(II)
A_{HJ}	0.309	0.307	0.273	0.273
B_{HJ}	0.345	-0.015	0.143	-0.110
R^2	0.8693	0.7909	0.8314	0.8231

3.2.5 Halsey Isotherm Model

Halsey isotherm model can be used to evaluate the multilayer adsorption system for metal ions adsorption at a relatively large distance from the surface and is expressed as [47]:

$$ln(q_e) = \left[\left(\frac{1}{n_H}\right)\ln(K_H)\right] - \left(\frac{1}{n_H}\right) ln\left(\frac{1}{C_e}\right) \qquad (9)$$

Where KH and nH are the Halsey constants, which can be evaluated from the slope and the intercept of the linear plot of $ln(q_e)$ *versus* $ln\left(\frac{1}{C_e}\right)$, respectively as shown in Figures 15 and 16. The related Halsey isotherm constants and coefficient of determination (R^2 values) are calculated and presented in Table 5. The high R^2 values as observed from Table 5 show an

excellent fit of the isotherm for the experimental adsorption data. This finding implies that Cu(II) and Cd(II) adsorption on both UBSH and MBSH obeys the Halsey isotherm model. Comparison of the values of linear regression coefficient (R^2) of the five examined isotherm models, revealed that the Freundlich and Halsey isotherm models gave much better fitting than the other three isotherm models (*i.e.*, Langmuir, Temkin and Harkins-Jura isotherms). Consequently, the adsorption behaviors of Cu(II) and Cd(II) ions on both surfaces can be well described using these two isotherm models.

Table 5. Halsey Isotherm Constants.

Constants	UBSH		MBSH	
	Cu(II)	Cd(II)	Cu(II)	Cd(II)
K_H	1.927	4.199	2.549	4.538
n_H	1.383	1.280	1.178	1.159
R^2	0.9852	0.9894	0.9950	0.9954

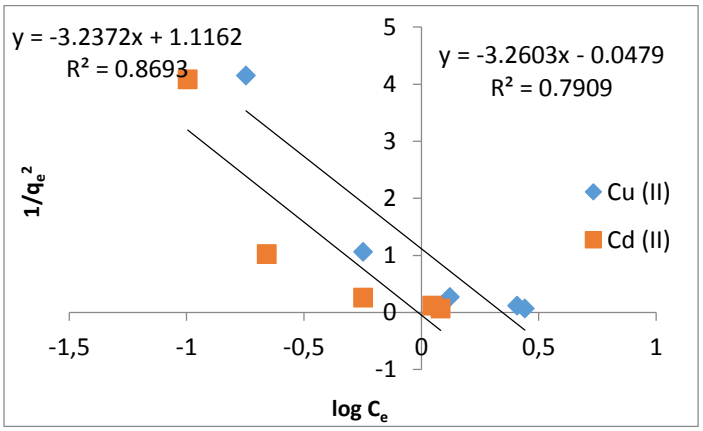

Figure 13. Plot of the Harkins-Jura isotherm model for Cu(II) and Cd(II) adsorption on UBSH.

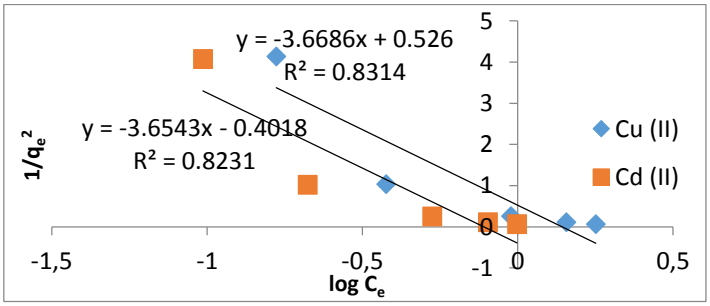

Figure 14. Plot of the Harkins-Jura isotherm model for Cu(II) and Cd(II) adsorption on MBSH.

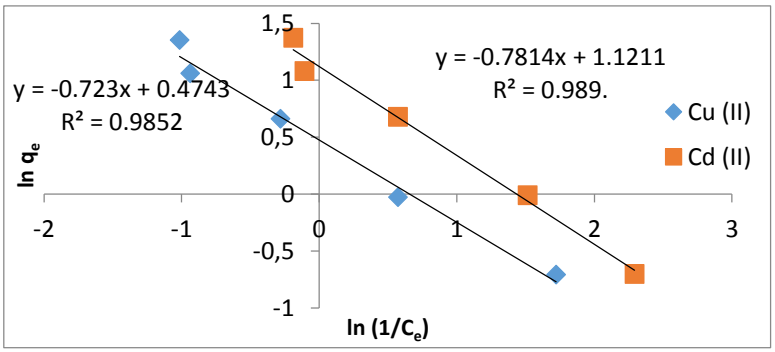

Figure15. The Halsey isotherm model for Cu (II) and Cd(II) adsorption onto UBSH.

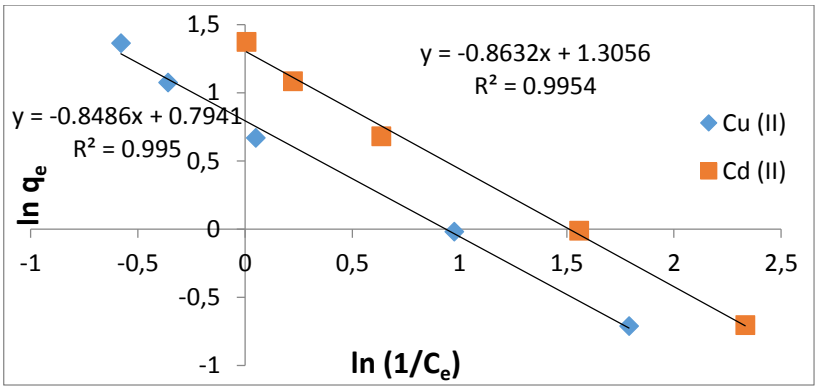

Figure 16. The Halsey isotherm model for Cu(II) and Cd(II) adsorption onto UBSH.

4. CONCLUSION

In this present investigation, the effects of adsorbent particle size, adsorbent dose and initial metal ion concentrations were studied. The results generally showed an increase in percentage removal and a corresponding decrease in adsorption capacity with increase in adsorbent dosage. Results further show an increase in adsorption capacity as the adsorbent particle size decreased. Mercaptoacetic acid modification of the adsorbent led to further enhancement in the removal efficiency of the metal ions by the adsorbent. Five different isotherm models viz; the Langmuir, Freundlich, Temkin, Harkins-Jura, and Halsey models were applied to the experimental data. The Freundlich and the Halsey models gave the best description for the adsorption data while the other three isotherm models gave a fairly good description for the experimental data. Fitting of the adsorption data into Freundlich model shows that the forces of adsorption may follow the physical mode. The adsorption heat calculated from the Temkin isotherm equation was restricted within 1.314–2.202 kJ $mol^{-1.}$ Results obtained from this study clearly showed that the adsorbent showed a better removal for Cd(II) than Cu(II) ions from the aqueous solutions. Chemical modification of the adsorbent further enhanced the adsorption capacity. This study has shown that the use of *Treculia africana* for adsorption of Cu(II) and Cd(II) ions is technically feasible and eco-friendly.

5. REFERENCES AND NOTES

[1] Kinhikar, V. R. *Res. J. Chem. Sci.* **2012,** *2*, 6.

[2] World Health Organization. Guideline for drinking –water quality. In: Chemical Fact Sheet. World Health Organization: Geneva, **2004**.

[3] Kawarada, K.; Haneishi, K.; Lida, T. *Wood Ind.* **2005**, *60*, 398.

[4] Farooq, U.; Kozinski, J. A.; Khan, M. A.; Athar, M. *Biores. Technol.* **2010**, *101*, 5043. [CrossRef]

[5] Sousa, F. W.; Oliveira, A. G.; Ribeiro, J. P.; Rosa, M. F.; Keukeleire, D.; Nascimento, R. F. *J. Environ. Manage.* **2010**, *91*, 1634. [CrossRef]

[6] Keshinkan, O.; Goksu, M. Z. I.; Basibuyuz, M.; Forster, C. F. *Bioresource Technol.* **2004**, *92*, 197. [CrossRef]

[7] Bai, R. S.; Abraham, T. E. *Water Res.* **2002**, *36*, 1224. [CrossRef]

[8] Nuhoglu, Y.; Oguz, E. *Process Biochem.* **2003**, *38*, 1627. [CrossRef]

[9] Brown, P.; Jefcoat, V.; Parrish, D.; Gill, S.; Graham, E. *Adv. Environ. Res.* **2000**, *4*, 19. [CrossRef]

[10] Chuah, T. G.;Jumasiah, I.; Azni, S.; Katayon, S.; Thomas Choong, S. Y. *Desalination* **2005**, *175*, 305. [CrossRef]

[11] Ho, Y. S; Mckay, G. *Water Res.* **2000**, *34*, 735. [CrossRef]

[12] Onwu, F. K.; Ngele, S. O.; Elom, N. I. *Int. J. Chem. Appl.* **2014**, *6*, 69.

[13] Dada, A. O; Ojediran, J. O.; Abiodun, P. O. *Adv. Physical Chem.* **2013**, *2013*, 1.

[14] Yu, B.; Zhang, V.;Shukla, A.; Shukla, S. S.; Dorris, K. L. *J. Hazard. Mater.* **2001**, *B84*, 83. [CrossRef]

[15] Hossain, M. A.; Rahman, M. A. *Orbital: Electron. J. Chem.* **2012**, *4*, 187. [Link]

[16] Wang, S.; Peng, Y. *Chem. Eng. J.* **2010**, *156*, 1. [CrossRef]

[17] Ouki, S. A.; Neufeld, R. D. *J. Chem. Tech. Biotechnol.* **1997**, *70*, 3. [CrossRef]

[18] Mohan, D.; Singh, K. P. *Water Res.* **2002**, *36*, 2304. [CrossRef]

[19] Hu, Z.; Lei, L.; Li, Y.; Ni, Y. *Sep. Purif. Technol.* **2003**, *31*, 13. [CrossRef]

[20] Rivera-Utrilla, J.; Bautista-Toledo, I.; Ferro-Garcia, M. A.; Moreno-Castilla, C. *Carbon* **2003**, *41*, 323. [CrossRef]

[21] Periera, M. F. R.; Soares, S. F.; Orfao, J. M. J.; Figueiredo, J. L. *Carbon* **2003**, *41*, 811. [CrossRef]

[22] Marquez, G. E.; Ribeiro, M. J. P.; Ventura, J. M.; Labrincha, J. A. *Ceram. Int.* **2004**, *30*, 111. [CrossRef]

[23] Alfin, O.; Ozbelge, H. O.; Dogu, T. *J. Colloid Interf. Sci.* **1998**, *198*, 130. [CrossRef]

[24] Zhang, V.; Asakura, T.; Uchiyama, G. *React. Funct. Polym.* **2003**, *57*, 67. [CrossRef]

[25] Atia, A.; Donia, A. M.; Abou-El-Enein, S. A.;Yousif, A. M. *Sep Purif. Technol.* **2003**, *33*, 295. [CrossRef]

[26] Jong, S. K.; Soonwoo, C.; Jongheop, Y. *Korean J. Chem. Eng.* **2000**, *17*, 118. [CrossRef]

[27] Tikhomirova, T. I.; Fadeeva, V. I.; Kudryantsev, G. V.; Nesterenko, P. N. *Talanta* **1991**, *38*, 267. [CrossRef]

[28] Mortazavi, K; Ghaedi, M.; Roosta, M.; Montazero, Z. M. *Indian J. Sci. Technol.* **2012**, *5*, 1893.

[29] Camila, G. P.; Eder, C. L.; Leliz, T. A.; Nathalia, M. S.; Bruna, M. D; Jorge, L. B.; Tania, M. H. C.; Edilson, V. B. *Colloids Surf. A: A Physicochem. Eng. Aspects* **2008**, *316*, 297.

[30] Soliman, E. M.; Saleh, M. B.; Ahmed, S. A. *Anal. Chim. Acta* **2004**, *52*, 133. [CrossRef]

[31] Kumar, R.; Abraham, T. N.; Jain, S. K. *2nd International Conference on Environmental Science and Development* **2011**, *4*, 48.

[32] Wang, X.; Guo, Y.; Yang, L.; Han, M.; Zhao, J.; Cheng, X. *J. Environ. Anal. Toxicol.* **2012**, *2*, 1.

[33] Gupta, V. K.; Agarwal, S.; Saleh, T. A. *J. Hazard Mater.* **2011**, *185*, 17. [CrossRef]

[34] Chen, C.; Wang, X. *Ind. Eng. Chem. Res.* **2006**, *45*, 9144. [CrossRef]

[35] Pyrzynska, K.; Bystrzejewski, M. *Colloids Surf. A* **2010**, *362*, 102. [CrossRef]

[36] Rao, G. P.; Lu, C.; Su, F. *Sep. Purif. Technol.* **2007**, *58*, 224. [CrossRef]

[37] Farghali, A. A.; Bahgat, M.; Allahm, E. A.; Khedr, M. H. *J. Basic Appl. Sci.* **2013**, *2*, 61.

[38] Okieimen, F. E.; Okundaye, J. N. *Biol. Wastes* **1989**, *30*, 225. [CrossRef]

[39] Babel, S.; Kurniawan, T. A. *Chemosphere* **2004**, *54*, 951. [CrossRef]

[40] Nomanbhay, S. M.; Palanisamy, K. *Electron. J. Biotechnol.* **2005**, *8*, 43. [CrossRef]

[41] Li, Y.; Du, Q.; Wang, X.; Zhang, P.; Wang, D.; Wang, Z.; Xia, Y. *J. Hazard. Mater.* **2010**, *183*, 583. [CrossRef]

[42] Ahalya, N.; Kanamadi, R. D.; Ramachandra, T. V. *Electron. J. Biotechnol.* **2005**, *8*, 258. [CrossRef]

[43] McKay, G; Blair, H. S.; Gardener, J. R. *J. Appl. Polym. Sci.***1982**, *27*, 3043. [CrossRef]

[44] Anusiem, A. C. I; Onwu, F. K.; Ogah, S. P. I. *Int. J. Chem.* **2010**, *20*, 265.

[45] Song, C.; Wu, S.; Cheng, M.; Tao, P.; Shao, M.; Gao, G. *Sustainability* **2014**, *6*, 86. [CrossRef]

[46] Malkoc, E.; Nuhoglu, Y. *Chem. Eng. Process.* **2007**, *46*, 1020. [CrossRef]

[47] Liu, J.; Wang, X. *Sci. World J.* **2013**, *2013*, 1.